HHS Public Access

Author manuscript

Pharmacol Res. Author manuscript; available in PMC 2022 January 01.

Published in final edited form as:

Pharmacol Res. 2021 January ; 163: 105272. doi:10.1016/j.phrs.2020.105272.

ARGININE VASOPRESSIN RECEPTOR 2 ACTIVATION PROMOTES MICROVASCULAR PERMEABILITY IN SEPSIS

Ernesto Lopez, MD, PhD[1], **Satoshi Fukuda, MD**[1], **Katalin Modis, PharmD, PhD**[1,2], **Osamu Fujiwara, MD**[1], **Baigal Enkhtaivan, MD**[1], **Raul Trujillo-Abarca, MD**[1], **Koji Ihara, MD**[1,3], **Francisco Lima-Lopez, MD**[1,2], **Dannelys Perez-Bello, PhD**[1], **Csaba Szabo, MD, PhD**[1,4], **Donald S. Prough, MD**[1], **Perenlei Enkhbaatar, MD, PhD, FAHA**[1]

[1] Department of Anesthesiology, University of Texas Medical Branch, Galveston, TX, USA [2] Department of Surgery, University of Texas Medical Branch Galveston, TX, USA [3] Department of Plastic and Reconstructive Surgery, Kagoshima City Hospital, Kagoshima, Japan [4] Department of Pharmacology, University of Fribourg, Fribourg, Switzerland

Abstract

Methicillin-resistant *Staphylococcus aureus* (MRSA) sepsis is a severe condition associated with vascular leakage and poor prognosis. The hemodynamic management of sepsis targets hypotension, but there is no specific treatment available for vascular leakage. Arginine vasopressin (AVP) has been used in sepsis to promote vasoconstriction by activating AVP receptor 1 (V_1R). However, recent evidence suggests that increased fluid retention may be associated with AVP receptor 2 (V_2R) activation worsening the outcome of sepsis. Hence, we hypothesized that inhibition of V_2R activation ameliorates the severity of microvascular hyperpermeability during sepsis. The hypothesis was tested using a well-characterized and clinically relevant ovine model of MRSA pneumonia/sepsis and *in vitro* assays of human lung microvascular endothelial cells (HMVECs). *In vivo* experiments demonstrated that the treatment of septic sheep with tolvaptan (TLVP), an FDA-approved V_2R antagonist, significantly attenuated the sepsis-induced fluid retention and markedly reduced the lung water content. These pathological changes were not affected by the treatment with V_2R agonist, desmopressin (DDAVP). Additionally, the incubation of cultured HMVECs with DDAVP and DDAVP along with MRSA significantly increased the paracellular permeability. Finally, both the DDAVP and MRSA-induced hyperpermeability was significantly attenuated by TLVP. Subsequent protein and gene expression assays determined that the V_2R-induced increase in permeability is mediated by phospholipase C beta (PLCβ) and the potent permeability factor angiopoietin-2. In conclusion, our results indicate that the activation of the AVP-V_2R axis is critical in the pathophysiology of severe microvascular hyperpermeability during Gram-positive sepsis. The use of the antagonist TLVP should be considered as adjuvant

Author for correspondence: Perenlei Enkhbaatar MD., PhD., FAHA, Professor, Department of Anesthesiology, The University of Texas Medical Branch, 601 Harbor Side Dr. BLDG 21, Room 3.100C, Galveston, TX 77555, Tel: 409-747-0096, peenkhba@utmb.edu.

Author's contributions: Conception and design: EL, PE; *In vivo* experiments: EL, SF, OF, BE, KI, FL, PE; Biochemical and *in vitro* assays: EL, KM, BE, RT, DP; Analysis and interpretation: EL, SF, KM, OF, BE, RT, KI, FL, DP, CS, DSP, PE; Drafting the manuscript: EL, KM, PE; Critical revision of the manuscript: EL, SF, KM, CS, DSP, PE;

Conflict of interest disclosures: None

treatment for septic patients. The results from this clinically relevant animal study are highly translational to clinical practice.

Keywords

Sepsis; shock; tolvaptan; microvascular hyperpermeability; endothelium

1. INTRODUCTION

Sepsis is a global public health problem. Annually, it is estimated to affect more than 18 million people worldwide (1), including >700,000 people in the United States (2). The high incidence of sepsis is concerning given the fact that the mortality can be as high as up to 80% when septic shock is present (1, 3–6).

Vascular leakage, a major detriment leading to mortality, is one of the main challenges in the management of sepsis and septic shock. The damaged endothelium along with the upregulated systemic immune response plays a critical role in the pathophysiology of sepsis-induced vascular hyperpermeability. The diffuse stimulation of the endothelium not only increases the release of inflammatory mediators, but it also affects the vascular permeability primarily by disrupting the endothelial cell junctions (7).

In the past, arginine vasopressin (AVP) was used as an adjuvant vasopressor via its V_1R activation properties. However, results from the Vasopressin and Septic Shock Trial (VASST), demonstrated that the effects of AVP proved to be inefficient to reduce the overall mortality rate of septic patients (8).

As suggested by several studies, activation of V_2R during sepsis is detrimental (9). In endothelial cells, V_2R activation has been linked to an increased release of von Willebrand Factor (vWF) and nitric oxide (NO), as well as an elevated activity of tissue plasminogen activator (TPA) and P-selectin. We have previously demonstrated, in ovine sepsis models, that treatment with a selective V_1R agonist provides therapeutic benefits in contrast to AVP (10). Interestingly, adjunct treatment with selective V_2R agonist abolished the therapeutic effects of V_1R agonist on vascular hyperpermeability (9, 10). In the same context, a worsening fluid overload, organ dysfunction and mortality has being shown associated with an increase in circulating angiopoietin-2 (11, 12), which is colocalized with vWF in the Weibel-Palade bodies (WPBs) and may be released simultaneously by V_2R activation (13).

We hypothesized that V_2R activation promotes vascular hyperpermeability during sepsis. To test our hypothesis, we evaluated the effect of tolvaptan (TLVP), an FDA-approved V_2R antagonist in a highly translational ovine model of smoke inhalation (SI) and methicillin-resistant *Staphylococcus aureus* (MRSA) pneumonia/sepsis. Downstream mechanisms were explored using *in vitro* assays conducted in human lung microvascular endothelial cells (HMVEC). To our knowledge, the present study is the first report that describes the beneficial role of V_2R inhibition using a clinically relevant large animal model in MRSA sepsis.

2. MATERIAL AND METHODS

2.1. Animals

We used adult female merino sheep with a mean body weight of 33.7 ± 3.1 kg. The use of animals and procedures were approved and supervised by the Institutional Animal Care and Use Committee of the University of Texas Medical Branch and were in compliance with the guidelines established by the U.S. Department of Agriculture Animal Welfare Act and the National Institutes of Health/ Office of the Laboratory Animal Welfare.

2.2. Human lung microvascular endothelial cells (HMVECs)

Commercially available primary HMVECs (Cat# 540–05a, Cell Applications, Inc., San Diego, CA) were subculture using microvascular endothelial growth media (Cat# 111–500, Cell Applications, Inc., San Diego, CA) according to vendor's instructions. In brief, cryopreserved cells were revived from passage 3, expanded and used for the experiments between passage 5 and 7. The expression of PECAM-1 (also called CD31), VEGF and von Willebrand factor were assessed.

2.3. Drugs

In vivo experiments: Desmopressin (DDAVP) (Ferring Pharmaceuticals, Saint Prex, Switzerland); Up to 32 μg of DDAVP was diluted in 1 L of 0.9% sodium chloride solution (NS: normal saline). Tolvaptan (TLVP) (Biorbyt Ltd; Cambridge, UK); Up to 400 mg of TLVP was dissolved in 1 L of NS with 5% polysorbate-80 and 0.1% dimethyl sulfoxide (DMSO). The formulations were prepared freshly on the day of the experiment and were adjusted to the body weight.

In vitro assays: DDAVP (Cat#SC-391876, Santa Cruz Biotechnology, Dallas, Texas) was re-suspended in water to reach a concentration of 3000 nM, and the aliquots were frozen and stored at −20 °C until the day of the experiment. Using the same preparation as in the *in vivo* experiments, 1 M TLVP was prepared on the day of the experiment and diluted in culture media to reach 10 nM concentration in the assay. The effective concentrations of DDAVP and TLVP were selected in agreement with previous work and results of dose-response tests performed in our laboratory (14–16). Recombinant Human VEGF (Cat#100–20, Peprotech, Rocky Hill, NJ) was re-suspended in culture media containing 0.1% fetal bovine serum (FBS) (Cat#F2442, Sigma-Aldrich, St. Louis, NO) as vehicle. Aliquots of 1 μg/mL were frozen and stored at −20 °C until the day of the experiment. U73122 (Cat#1268, TOCRIS, Bristol, United Kingdom) was re-suspended in DMSO to reach a concentration of 5 mM, and the aliquots were frozen and stored at −20 °C. On the day of the experiment, an aliquot solution was dissolved in culture media to reach 1:50,000 dilution and a concentration of 100 nM.

2.4. Methicillin-Resistant Staphylococcus Aureus (MRSA)

Commercially available MRSA (Strain USA300 / TCH1516, ATCC, Manassas, VA) were grown in an orbital shaker incubator at 37 °C with agar media. A standard curve was performed to correlate the optical density (OD) with the bacteria growth and determine the colony-forming units (CFU) per mL (CFU/mL). The day of the experiment, the OD of

bacterial suspension was measured, and the concentration of bacteria determined based on the OD *vs.* CFU/mL standard curve obtained previously. Dilutions were prepared according to the number of bacteria required. Then, the bacterial suspension was washed twice; centrifuge at 4,000 RPM (Centrifuge 5810R, Eppendorf, Hamburg, Germany) for 10 minutes and re-suspended in phosphate-buffered saline (PBS). The final concentration for the *in vivo* experiments was 3.5×10^{11} CFU suspended in 30 mL of PBS, replicated from our recent work (17) and adjusted from the original model using a different MRSA strain (18). For *in vitro* assays, the solution containing 2×10^{9} CFU suspended in 5 mL of PBS was used as stock. The proportion of the stock solution was mixed with culture media before the bacteria were exposed to the endothelial cells. The optimal concentration of bacteria used in our assays was determined previously by our laboratory using a multiplicity of infection (MOI) of 15 in relation to the number of endothelial cells(19). For the vascular permeability assay, the concentration applied was 3×10^{6} CFU, and for the gene expression assays was 1.2×10^{7} CFU.

2.5. *In vivo* ovine MRSA sepsis model

2.5.1. Surgical preparation: The animals were surgically prepared according to our well-characterized *in vivo* model (20). Under rigorous aseptic conditions, the animals were surgically prepared to place catheters in the pulmonary artery (79F Swan-Ganz, Edwards Lifesciences LLC, Irvine, CA), the femoral artery (16-GA, 24 inches; Becton Dickinson, Franklin Lakes, NJ) and the left atrium (Silastic catheter, 0.062-in. inner diameter, 0.125-inches. outer diameter; Dow-Corning, Midland, MI) for continuous hemodynamic monitoring, intermittent blood sampling and administration of drugs and fluid. The procedure was performed under general anesthesia using 1.7 mg buprenorphine (Buprenorphine SR, ZooPharm, Windsor, CO) for pain control, 800 mg ketamine (KetaVed, VEDCO, St. Joseph, MO) for anesthesia induction and 2 to 5 % isoflurane (IsoSol, VEDCO, St. Joseph, MO) for anesthesia maintenance.

2.5.2. Injury: After the surgery, the animals were allowed to recover for five days under analgesia and with *ad libitum* access to water and food in our translational intensive care unit (TICU) facility. On the day of the experiment, baseline measurements were taken followed by deep anesthesia and analgesia, insertion of a cuffed tracheostomy tube (10 mm diameter, Shiley, Irvine, CA, USA) and a urinary bladder catheter (Foley Catheter, 14Fr; BARDEX®, Covington, GA). Then, anesthetized animals were subjected to insufflation of 48 breaths of cooled cotton smoke and instillation of MRSA (3.5×10^{11} CFU) into the lungs by bronchoscope via the tracheostomy tube. After the injury, the animals were placed on mechanical ventilation and monitored 24 hours in a conscious state (17, 18, 21). During the study period, animals were humanely euthanized and count as a fatality if they met the standardized euthanized criteria (PaO_2 <50 mmHg, MAP < 50mmHg or CO_2 < 90 mmHg) or after 24 hours (22). The organs were processed immediately, as previously described (21, 23). The animal model employed, as previously described, is a double (SI plus MRSA inoculation). Additionally, the animals were supported with mechanical ventilation. We have shown that the model closely mimics the features of clinical sepsis (17, 18). MRSA-pneumonia can occur during the hospitalization (hospital-acquired pneumonia [HAP]) in

patients with mechanical ventilation for extended period due to respiratory failure (viral pneumonia, smoke inhalation etc. (24).

2.5.3. Grouping and treatments: Twenty-five animals were randomly divided into one of the four study groups. Sham group (n=6) was not subjected to either SI or MRSA but did receive continuous mechanical ventilation and treatment with 35 mL/hour of NS. The SI +MRSA group (n=7) received the injury and the same treatment as Sham. DDAVP (n=6) and TLVP (n=6) groups were injured and received 38 ng/kg/hour DDAVP and 435 μg/kg/hour TLVP, respectively. The treatments were administered an hour after the injury as a continuous IV infusion over 23 hours. DDAVP dose was chosen based on previous studies from our laboratory, showing a V_2R stimulation comparable to 0.03 U/minute AVP (10, 25). TLVP dose was adapted from published studies (26, 27).

2.5.4. Resuscitation and ventilatory management: After the injury, sheep were awakened and placed on mechanical ventilation (AVEA™ Ventilator; CareFusion, Yorba Linda, CA). The cardiopulmonary variables were monitored for 24 hours in a conscious state. A volume/pressure control mode was used with positive end-expiratory pressure (PEEP) of 5 cmH_2O and a tidal volume (V_t) of 12 mL/kg. During the first 3 hours after the injury, the FiO_2 was maintained at 100% in all animals, and then titrated to an arterial PaO_2 close to 100 mmHg. The respiratory rate started at 20 breaths/minute in all animals and was further adjusted to ensure a $PaCO_2$ between 25 and 35 mmHg. The animals were fluid resuscitated with 2 mL/kg of Lactated Ringer's (LR) as starting rate, and then titrated based on a standard protocol to maintain the hematocrit ± 3% from baseline values (18). Administration of resuscitation fluid was given intravenous (IV) with an infusion pump (MicroMacro XL3 Plum XL3, Abbot Laboratories, Chicago, IL). Urine output was continuously collected with the urinary bladder catheter (Foley Catheter, 14Fr; BARDEX®, Covington, GA) for an accurate assessment of the fluid balance.

2.5.5. Assessment of hemodynamics: Central venous pressure (CVP), pulmonary artery pressure (PAP), pulmonary microvascular capillary pressure (PcP), left atrium pressure (LAP), mean arterial pressure (MAP) and heart rate (HR) were recorded by hemodynamic monitors (IntelliVue MP50, Philips Medizin Systeme Boeblingen, Boeblingen, Germany) via pressure transducers connected to the vascular catheters. The lung hydrostatic pressure was calculated with a standard equation: $P_c = (0.6 \times PcP) + (0.4 \times PAP)$. The thermodilution technique was used to determine cardiac output (PX1800, Edwards Lifesciences LLC, Irvine, CA) and core body temperature.

2.5.6. Pulmonary mechanics and gas exchange: The pulmonary function was evaluated with the pulmonary oxygenation index (OI), which integrates the PaO_2/FiO_2 ratio and the mean airway pressure (P_{aw}). These parameters were determined with equations used in the past (28, 29).

2.5.7. Blood parameters and biomarkers: Blood samples were taken every three hours, processed as fresh heparinized blood or as plasma to store at −20 °C until termination of the study. Fresh heparinized blood was used to determine PO_2, CO_2, pH, carboxyhemoglobin (COHb), and hemoglobin using a blood gas analyzer (GEM Premier

3000; Instrumentation Laboratories, Lexington, MA). For determination of hematocrit and white blood cells (WBC), a hematology system (Hemavet 850™; Drew Scientific, Inc., Oxford, CT) was used.

2.5.8. Simple Western immunoblotting of heart tissues: Sheep heart tissue was homogenized in tissue protein extraction reagent (T-PER™) (Cat#78510, Thermo Fisher Scientific Inc., Waltham, MA). Tissue homogenization solutions were supplemented with proteinase inhibitor cocktail (Cat# P8340, Sigma-Aldrich, St. Louis, MO), and phosphatase inhibitors (Phenylmethanesulfonyl fluoride; Sigma-Aldrich, St. Louis, MO). The samples were analyzed with a Simple Western instrument for protein quantification (Simon™, ProteinSimple, Santa Clara, CA) using a protein quantification kit (Rabbit 12–180 kDa master kit for Simon, Cat#Simon-01–01, ProteinSimple, Santa Clara, CA). In short, we loaded a 384-well plate using 5 μg of protein diluted in Laemmeli denaturing loading buffer (Biorad, Hercules, CA) mixed with fluorescent standards and primary anti-angiopoietin-2 antibody (Cat# ab8452, Abcam, Cambridge, MA) diluted in antibody diluent buffer at a 1:20 ratio and mixed with anti-actin (Cat#A2066, Sigma-Aldrich, St. Louis, NO) diluted at the same ratio. The chemiluminescence signal was integrated and analyzed with Compass software Version 2.7.1 (ProteinSimple, Santa Clara, CA)(30).

2.5.9. Lung wet-to-dry weight ratio: Lung water content was determined by measuring lung wet-to-dry ratio (W/D); 960 ± 182 mg of lung tissue were weighed before and after the water evaporated at 60 °C in a vacuum oven (23).

2.6. In vitro assays using HMVECSs

2.6.1. Vascular permeability assay: An *in vitro* vascular permeability assay was established and optimized using a previously described method with minor modifications (31). Three μm pore size transwell inserts (Cat# 354575, Thermo Fisher Scientific Inc., Waltham, MA) were coated with sterile extracellular matrix (Matrigel™, Cat# 354234, Thermo Fisher Scientific Inc., Waltham, MA) and incubated at 37 °C. Then, 200,000 cells in passage 5 were seeded during two consecutive days. The cells were then allowed to form a tight monolayer for 48 hours. In this model, the extracellular matrix over the multi-pore membrane represents the basal membrane, and the microvascular endothelial cells seeded at a high concentration forms a tight endothelial monolayer. The system together represents a microvascular endothelial barrier model previously detailed by our research group (32). The endothelial barrier was further challenged with different pharmacological agents, MRSA or the combination of both.

On the day of the study, the culture media was aspirated from the wells and the pretreatment (TLVP or starvation media) was added. Thirty minutes later, it was replaced by the indicated treatment. Fluorescent dextran (FITC-Dextran, Thermo Fisher Scientific Inc., Cat# D-3306, Waltham, MA) at a concentration of 10 μg/mL was added to the lower chamber in combination with the treatment. Every 30 minutes after the treatment was initiated, 20 μL of supernatant media were collected from the upper chamber and placed in a black plate (Costar, Cat#06–443-2, Thermo Fisher Scientific Inc., Waltham, MA) containing 90 μL of water per well (Figure 2.3.1.). The amount of FITC-Dextran in the media was quantified

using a fluorometer reader (Powerwave HT, Biotek, Winooski, VT) with excitation of 485 nm and emission of 535 nm.

The concentrations of DDAVP and TLVP were adapted from the work previously done (14–16) and confirmed in our laboratory with a dose-response test (data not shown). Treatments were conducted in starvation media applying 1 mL for the lower chamber and 300 μL for the upper chamber. For starvation media, we used basal media (Cell Applications Inc., Cat#100–500, San Diego, CA) with 1% of FBS (Cat#F2442, Sigma-Aldrich, St. Louis, NO). For Vehicle, we used starvation media with 0.001% DMS0 and 0.01% polysorbate 80. For the wells exposed to MRSA, we targeted an MOI of 15; therefore, we applied 3×10^6 CFU MRSA suspended in 50 μL of starvation media. The smaller volume used over the insert facilitates the interaction between the endothelial cells and the bacteria. Cells and bacteria were allowed to interact for 6 hours before the permeability was evaluated with the FITC-Dextran polymers.

2.6.2. Electrical resistance assay: Adapted from previous work (32), HMVECs were seeded in a 96-well cell culture plate equipped with gold electrodes (E-plate, Cat#05232376001, ACEA BIO, San Diego, CA) at a concentration of 15,000 cells per well. The electrical resistance was determined by measuring electrical impedance every 15 minutes by cell-microelectronic sensing (XCELLigence™ RTCA, ACEA BIO, San Diego, CA). When cells became confluent (indicated by a plateau of electrical impedance), the cells were incubated with starvation media for 2 hours, followed by replacement with media containing VEGF, DDAVP, TLVP, TLVP+DDAVP or only starvation media. The electrical resistance continued to be recorded every 15 minutes for 12 hours. The drugs were applied at the same concentration as described for the vascular permeability assay.

2.6.3. Lactate dehydrogenase (LDH) assay: As previously described (33), 30 μL of culture media were collected at each time point (1, 3 and 6 hours for this study) and stored at 4 °C until the last sample was collected. The culture media sample was mixed with 100 μl of LDH assay reagent constituted with 85 mM lactic acid, 1040 mM nicotinamide adenine dinucleotide, 224 mM N-methylphenazonium methyl sulfate, 528 mM 2-(4-iodophenyl)-3-(4-nitrophenyl)-5-phenyl-2H-tetrazolium chloride and 200 mM Tris-pH 8.2. Immediately after the culture media was mixed with the LDH reagent, the OD was read with a monochromator-based reader (Powerwave HT, Biotek, Winooski, VT) at 492 nm during 15 minutes of incubation at 37 °C. Using the Michaelis-Menten formula, the LDH activity was determined by calculating the maximum velocity achieved by the system (V_{max}). The higher the $\%V_{max}$ indicated by the assay, the higher the LDH activity in the cell culture, which correlates with the degree of cell death.

2.6.4. Protein determination in cell culture supernatant: HMVECs were allowed to grow until confluence in 25 cm^2 cell culture flasks. On the day of the experiment, the culture media was replaced with 2.6 mL of starvation media with or without treatment. Then, the supernatant was collected, mixed with 1.4 mL of PBS and 40 μL of proteinase inhibitor cocktail (Cat# P8340, Sigma-Aldrich, St. Louis, MO), added into a 4 mL ultra-filter for protein concentration (Amicon Cat# UFC8–003-24, EMD Millipore, Darmstadt Germany) and centrifuge for 60 minutes at 4,000 RPM (Centrifuge 5810R, Eppendorf,

Hamburg, Germany). Approximately 150 μl of concentrated supernatant was achieved with this method, which represents a 27-fold concentration increase. The testing concentration was 300 nM DDAVP and was administered for 1, 3, or 6 hours. Culture media without exposure to cells was also concentrated under the same conditions and was used as an additional control (negative control). This negative control is essential because the protein of interest, angiopoietin-2, is often found in the culture media. The protein concentration in the concentrated samples was determined with a BCA protein assay kit (Thermo Fisher Scientific Inc., Cat#23225, Waltham, MA) and then diluted in PBS to a concentration of 1.4 μg/μL. Finally, the concentration of angiopoietin-2 was determined with simple Western immunoblotting as described above. In this experiment, angiopoietin 2 was undetected in the negative control samples.

2.6.5. Quantitative real-time polymerase chain reaction: Following the different experimental treatments, RNA was isolated using an RNA isolation kit (RNeasy® Mini Kit, Cat# 74106, Qiagen, Valencia, CA). Briefly, culture media was aspirated, and lysis buffer was applied to the culture plates at a concentration of 79 μL/cm^2. The cell lysate was collected and placed into a centrifuge tube, mixed with 70% ethanol (1:1 concentration) vortex for 2 minutes and transferred into a spin column and processed as indicated by the manufacturer. The RNA was diluted in RNase-free H_2O, 0.075 μL of H_2O for each μL of cell lysate used. The RNA concentration and quality were determined by measuring the OD with a Nanodrop spectrophotometer (Biotek, Winooski, VT).

To convert RNA into cDNA, 500 ng of RNA diluted in 16 μL of RNase-free H_2O were mixed with 4 μL of iScript™ RT supermix (Cat# 170–8841, Bio-Rad, Hercules, CA). The reaction mixture was incubated using a thermal cycler (T100, Bio-Rad, Hercules, CA) with standard manufacturer settings (5 minutes at 25 °C, 30 minutes at 42 °C and 5 minutes at 85 °C).

To quantify the expression of the genes of interest, we performed quantitative real-time polymerase chain reaction (RT-qPCR) using PrimePCR™ assays previously validated (Cat# 10025636, Bio-Rad, Hercules, CA) and optimized based on previous studies (34). Each sample was measured in duplicate using a 10 μL reaction containing 4 μL cDNA [2.5 ng/μL], 5 μL SsoAdvanced™ Universal SYBR® Green Supermix (Cat# 172–5270, Bio-Rad, Hercules, CA) and 1 μL PrimePCR™ assay [250 nM]. The 96-well plates were then run on a CFX96 RT-qPCR detection system (Cat# 10025636, Bio-Rad, Hercules, CA) with 30 seconds at 95°C for activation and 45 amplification cycles for 15 seconds at 95°C and 60 seconds at 60°C. Under these conditions, we measured the gene expression using PrimePCR™ assays for beta-actin (*ACTB*) (UniqueAssayID: qHsaCID0017615), angiopoietin-2 (*ANGPT2*) (UniqueAssayID: qHsaCED003626) and phospholipase beta 4 (*PLCB4*) (UniqueAssayID: qHsaCID0014933).

Relative normalized expression of genes of interest was determined by relative quantification using the threshold cycle (C_T) of interest gene vs. reference gene with the equation $C_T(\Delta\Delta C_T)$. The calculations were done using CFX Manager™ Software (Bio-Rad, Hercules, CA). ACTB was the reference gene, which showed to be unchanged after the treatments. TATA box binding protein (TBP) and hypoxanthine phosphoribosyltransferase 1

(HRP1) were also evaluated as reference genes, although CFX Manager™ determined higher efficacy for *ACTB*.

2.6.6. Multi-gene assays: As initial screening, we employed a multi-gene assay to screen for the 36 genes associated with g-protein-coupled receptors (p38 and JNK Regulation by G-Proteins, Cat#10025586 Bio-Rad, Hercules, CA). The cells were treated with 300 nM DDAVP or culture media only for 2 hours, and the RNA was isolated and converted to cDNA as described above. According to manufacturer instructions, we used 10 ng of cDNA per gene in a 20 μL reaction containing 10 μL cDNA [1 ng/μL] and 10 μL SsoAdvanced™ Universal SYBR® Green Supermix (Cat# 172–5270, Bio-Rad, Hercules, CA). The assay was run in a CFX96 RT-qPCR detection system (Cat# 10025636, Bio-Rad, Hercules, CA) and the results were analyzed with CFX Manager™ Software (Bio-Rad, Hercules, CA).

In subsequent experiments, we designed and assay taking the strongest upregulated gene signal shown by the multi-gene screening, *PLCB4*, along with *ANGP2* and the major genes implicated in the *MAPK* signaling pathway; *MAPK1* (UniqueAssayID: qHsaCED0042738), *MAPK3* (UniqueAssayID: qHsaCID0010939), *MAPK8* (UniqueAssayID: qHsaCID0010205), *MAPK9* (UniqueAssayID: qHsaCID0036311), *MAPK12* (UniqueAssayID: qHsaCID0004420), *MAPK13* (UniqueAssayID: qHsaCID0045741), *MAPK14* (UniqueAssayID: qHsaCID0043417), and *JUN* (UniqueAssayID: qHsaCID0018770). This multi-gene assay was replicated at multiple time points (30 minutes, 1 hour, 3 hours and 6 hours) after treatment with either DDAVP, MRSA or media only. The assay was conducted with a customized commercially available plate (Cat#10025217, Bio-Rad, Hercules, CA).

2.7. Statistical analysis

Results were compared by two-way analysis of variance using Sidak-Bonferroni post hoc test to evaluate differences between groups. Scores or measurements taken at a single timepoint were compared using Student *t* test for two groups and one-way analysis of variance with Sidak-Bonferroni post hoc test to compare three or more groups. The mortality among groups was compared using Fisher's exact test. All values are expressed as mean ± standard deviation (SD). Differences were considered significant when the p-value was smaller than 0.05. The statistical methodology was conducted accordingly (35).

3. RESULTS

In vivo:

3.1. The induced injury is comparable among SI+MRSA, DDAVP and TLVP groups—As detailed, prior to bacteria instillation, we insufflated cooled cotton smoke. The levels of COHb following SI were 71, 74 and, 82% for SI+MRSA, DDAVP, and TLVP groups, respectively. All statistically greater than the 5.4% showed in Sham group (Supplemental Table 1).

Six hours after the instillation of bacteria, the core body temperature and the heart rate increased in SI+MRSA, DDAVP, and TLVP groups and remained increased during the study.

SI+MRSA groups had a significant increase in fluid requirements at 6 hours, and DDAVP and TLVP groups at 9 hours compared to Sham group. The white blood cells (WBC) were also statistically diminished by 12 hours in all injured groups compared to Sham group. Platelet count was not assessed (Supplemental Table 1).

Mean arterial pressure (MAP) dropped in all injured groups showing a significant reduction in DDAVP and TLVP at 6 hours and in SI+MRSA at 9 hours vs. their baseline. In Sham group, MAP was unchanged during the study vs. its baseline except for a significant and transient increase at 3 hours (Supplemental Table 1).

All 25 studied animals survived the first 12 hours (SI+MRSA 7/7, DDAVP 6/6, TLVP 6/6 and Sham 6/6) and all groups exhibited clinical sepsis by this timepoint. Between 12 and 24 hours, SI+MRSA group had 4 fatalities (3/7 at 24 hours, 57% mortality rate). TLVP had one fatality between 21 and 24 hours (5/6 at 24 hours, 17% mortality rate). No mortality was recorded in DDAVP and Sham groups (6/6 and 6/6 at 24 hours). Differences in mortality were not statistically significant comparing DDAVP vs. SI+MRSA group (p=0.07) and TLVP vs. SI+MRSA group (p=0.2) using Fisher's exact test (Supplemental Figure 1).

3.2. TLVP treatment reduces the fluid requirement—LR rate was titrated to maintain hematocrit at baseline (± 3%). Sham group received 2,327 ± 814 mL of LR solution total for 24 hrs. SI+MRSA and DDAVP groups required a large amount of LR to maintain hematocrit throughout the study group (8,199 ± 2,334 mL and 6,837 ± 1,517 mL; p>0.05 vs. Sham). In contrast, the amount of fluid received by the TLVP group (4,606 ± 432) was not statistically different *vs.* Sham group. Comparing the injured groups, only the TLVP group required significantly less fluid than SI+MRSA (Figure 1A). The hematocrit and hemoglobin levels at 12 and 24 hours were statistically similar in all the groups, indicating that plasma volume was comparable.

3.3 The urinary output shows similarity in TLVP and SI+MRSA vs. reduced output in the DDAVP group—The accumulated 24 hours urinary output was 3,375 ± 1,058 mL in SI+MRSA, 2,165 ± 486 mL in DDAVP, 3,623 ± 788 in TLVP, and 2,366 ± 684 mL in Sham groups (P<0.05 vs. Sham). The urinary output in the DDAVP group was significantly lower *vs.* the TLVP group (P=0.01) (Figure 1B).

3.4. TLVP treatment reduces systemic fluid retention—The accumulated fluid volume was statistically greater in the SI+MRSA (126 ± 52 mL/kg, P<0.05) and DDAVP groups (142 ± 42 mL/kg, P<0.05) compared to the Sham group (1 ± 8 mL/Kg) at 24 hours, showing that in our model the amount of fluid retention was significantly elevated correlating well with the characteristics of critically ill septic patients (36). In the TLVP group, the retained amount of fluids was similar to the Sham group (30 ± 30 mL/Kg, at 24 hours, p=0.9) and lower than the DDAVP (P<0.001) and SI+MRSA groups (P<0.001) (Figure 1C).

3.5. TLVP treatment attenuates the increase in pulmonary resistance and lung water content—Compared to Sham, the PAP increased between 12 and 24 hours in the SI+MRSA group and between 15 and 24 hours in the DDAVP group. In the TLVP group,

an increase in PAP was significantly attenuated at 12 and 24 hours compared to SI+MRSA and had no statistical difference compared to Sham. (Figure 2A).

The PcP increased at 12 hours in the SI+MRSA group ($p<0.1$) and at 12, 15, 18, 21 and 24 hours in the DDAVP group ($p<0.05$, $p<0.01$, $p<0.05$, $p<0.0001$ and $p<0.01$ respectively) vs. Sham. In TLVP group, the PcP was significantly lower at 12 and 24 hours *vs.* SI+MRSA ($p<0.01$). No difference was found compared to Sham ($p=0.99$ and $p=0.18$, respectively) (Figure 2B).

Lung extravascular water content was determined by the changes in the wet-to-dry weight ratio (W/D). The SI+MRSA and DDAVP groups had significantly higher water content in the lung compared to Sham ($p<0.01$ and $p<0.05$, respectively). However, W/D in the TLVP group had no statistical difference *vs.* Sham group ($p=0.07$) (Figure 2C).

Lung function assessed by OI exhibited improvement in both DDAVP ($P<0.05$) and TLVP ($P<0.05$) groups *vs.* SI+MRSA at 12 hours. OI was similar in DDAVP ($p=0.8$) and TLVP ($p=0.8$) groups *vs.* SI+MRSA at 24 hours. Sham exhibited intact OI during the 24 hours study period with significant difference vs. SI+MRSA, DDAVP and TLVP at 24 hours ($p=0.16$) (Supplemental Figure 2).

In vitro:

3.6. V_2R agonist, DDAVP, increases the endothelial barrier permeability in vitro, as shown by electrical resistance and vascular permeability assays.—A dose-dependent study using an *in vitro* electrical resistance assay exhibited that DDAVP dose-dependently reduced the connectivity among the endothelial cells (Figure 1A). Similar effects were found with the addition of VEGF. However, TLVP prevented disruption of intercellular connectivity in DDAVP-challenged cells (Figure 1B). Complementary LDH-cytotoxicity assay demonstrated that the compounds used (at testing concentrations) do not promote acute cell death (Supplemental Figure 3).

Furthermore, these results were confirmed using a vascular permeability assay showing that treatment with DDAVP and VEGF (positive control) increased the passage of dextran across the HMVECs monolayer compared to Vehicle. However, pretreatment with TLVP significantly attenuated the DDAVP-induced increment in endothelial permeability. Treatment with TLVP did not cause any significant change in endothelial permeability *vs.* Vehicle (Figure 3C).

3.7. V_2R antagonist attenuates the endothelial hyperpermeability induced by MRSA.—Treatment of confluent HMVECs with MRSA augmented the passage of dextran through the endothelial monolayer compared to Vehicle. When the cells were pretreated with TVLP prior to the addition of MRSA, the amount of dextran across the monolayer did not differ from the Vehicle group. The co-incubation of MRSA plus DDAVP enhanced barrier hyperpermeability similar to the treatment with MRSA alone. These data suggest that MRSA treatment alone induced a maximal rate of endothelial permeability. Treatment with TLVP and subsequent addition of MRSA plus DDAVP showed a slight decrease in permeability with no statistical significance (Figure 3D).

3.8. The V_2R agonist, DDAVP, promotes the secretion of angiopoietin-2 protein and increases its gene expression in vitro.—

The angiopoietin-2 mRNA expression was significantly increased in HMVECs treated with DDAVP 2.3 ± 0.3-fold compared to Vehicle. To confirm that such mRNA upregulation indeed translates into a protein release, we measured angiopoietin-2 protein level in the HMVECs supernatant after a 6-hour treatment with DDAVP. The assay exhibited a significant 1.6-fold increase in angiopoieitin-2 level after DDAVP treatment vs. Vehicle (Figure 4A). These results demonstrated that increases in angiopoietin-2 mRNA expression translate into protein release; therefore, only mRNA was measured in subsequent experiments.

Notably, we found that angiopoietin-2 levels were significantly reduced in the heart tissue of sheep treated with TLVP compared to those that were treated with saline or DDAVP, suggesting that TLVP may have attenuated double hit injury (SI+MRSA)-induced vascular hyper-permeability by inhibiting angiopoietin-2. (Supplemental Figure 4).

3.9. TLVP pretreatment reduces the angiopoietin-2 mRNA expression in HMVECs compared to MRSA or DDAVP treatment.—

TLVP alone did not trigger a significant increase in angiopoietin-2 mRNA vs. Vehicle. Furthermore, when the cells were pretreated with TLVP prior to the addition of DDAVP, the increment in angiopoietin-2 mRNA was reduced and had no significant difference *vs.* the Vehicle group (Figure 4B).

Similar to DDAVP treatment, the level of angiopoietin-2 mRNA significantly increased in HMVECs exposed to MRSA 1.2×10^7 CFU (2.4 folds vs. Vehicle). Such upregulation of angiopoietin-2 induced by MRSA was slightly reduced with TLVP co-treatment (2 folds *vs.* Vehicle). MRSA-induced increases in angiopoietin-2 mRNA expression were further increased with DDAVP co-treatment (3.3 folds vs. Vehicle) (Figure 4C).

3.10. DDAVP treatment stimulates phospholipase C beta-4 (PLCB4) and angiopoietin-2 (ANGPT2) gene expressions in HMVECs.—

The initial screening of 36 genes after 2 hours of DDAVP treatment indicated that the phospholipase C beta-4 gene (*PLCB4*) was significantly upregulated (Figure 5A). Next, we measured the gene expression of PLCB4, *ANGPT2* and genes involved in the MAPK pathway at various time points (30 min, 1, 3 and 6 hours) after DDAVP or MRSA treatment. We found that none of the *MAPK* genes increased significantly with neither of the treatments or time points (Figure 5B, C, D, and E). *PLCB4* had a mild increase after 3 hours of treatment with MRSA and DDAVP (Figure 5D). At 6 hours, *PLCB4* was significantly increased in the DDAVP-treated group (Figure 5E). *ANGPT2* was elevated parallel to *PLCB4* at 3 and 6 hours (Figure 5D and E).

3.11. The DDAVP-induced upregulation of angiopoietin-2 gene expression is abolished after PLCβ4 inhibition.—

HMVECs treated with DDAVP promoted upregulation of *ANGPT2* expression as compared to Vehicle. However, PLCβ4 inhibitor (U73122) attenuated the DDAVP-induced *ANGPT2* upregulation, as shown by the lack of significant difference vs. the Vehicle group (Figure 5F).

4. DISCUSSION

The present findings demonstrate that the activation of V_2R plays a critical role in the pathophysiology of vascular hyperpermeability during Gram-positive sepsis. This concept is supported by the results of both *in vivo* and *in vitro* studies. First, septic sheep treated with V_2R antagonist tolvaptan (TLVP) significantly attenuated the sepsis-induced fluid retention and markedly reduced the lung water content. While these pathological changes were not attenuated by the treatment with V_2R agonist desmopressin (DDAVP). Second, the paracellular permeability of HMVECs subjected to DDAVP was significantly increased in a similar manner as the positive control group treated with VEGF. Finally, the hyperpermeability of HMVECs induced by either DDAVP or MRSA treatment was significantly attenuated by TLVP.

Our group previously described that the fluid retention was reversed in septic sheep treated with a selective V_1R agonist compared to other experimental groups treated with arginine vasopressin (AVP, V_1R, and nonselective V_2R agonist) or Vehicle (37). We also showed that co-treatment with DDAVP abolished the salutary effects of V_1R agonist on microvascular hyperpermeability, suggesting a possible involvement of V_2R activation in sepsis-induced vascular leakage (10). These findings were supported by a recent report by He *et al.* demonstrating superior outcomes, including decreased lung water content using Selepressin, a selective V_1R agonist (38). Taken together, the results of our present and previous studies demonstrate a critical role of V_2R activation in vascular leakage during ovine sepsis.

However, the mechanisms of how V_2R activation causes vascular hyperpermeability remain to be elucidated. As mentioned, treatment with TLVP significantly reduced lung water content and improved pulmonary oxygenation. Although these beneficial effects may be linked to the reduced pulmonary vascular resistance (P_cP and PAP) in TLVP-treated sheep, we do not exclude possible cardiac effects that positively impacted pulmonary function. Watanabe *et al.* have found, in clinical studies, a reduction in PAP after TLVP treatment for cardiac failure, attributing this salutatory effect to an improved cardiac function and/or an increase in circulating AVP (39, 40).

In recent years, angiopoietin-2 has gained particular attention among other sepsis-associated permeability factors due to its association with the severity and poor prognosis of septic patients (41–43), high specificity to disrupt the endothelial barrier (7, 44) and detrimental association with pulmonary hyperpermeability (45). It is well known that angiopoietin-2 is stored and secreted from the endothelial cells, specifically from the WPBs. This concept brings a particular interest for our study since vWF, a major resident of these intracellular vesicles, is released after V_2R activation (13, 14, 25, 46); therefore, it is feasible to speculate that activation of endothelial V_2R may promote the release of angiopoietin-2 as well. From the present *in vivo* findings, we showed that TLVP significantly reduced the level of angiopoietin-2 in cardiac tissue, suggesting that TLVP may have reduced microvascular hyperpermeability by inhibiting this potent permeability factor. This finding is of particular importance providing evidence for the therapeutic effect of V_2R blockage on the potent permeability factors such as angiopoietin-2.

We further investigated whether the activation of V_2R has a direct effect on vascular endothelium. First, by testing whether the V_2R-induced microvascular hyperpermeability is mediated by angiopoietin-2. Interestingly, angiopoietin-2 expression exhibited an increase in HMVECs incubated with the selective V_2R agonist, DDAVP, as shown by mRNA upregulation and confirmed by subsequent increase in protein levels. These findings suggest that V_2R activation may increase vascular permeability by stimulating angiopoietin-2 production. In support, pretreatment with the V_2R antagonist TLVP significantly inhibited the upregulation of angiopoietin-2 and, subsequently, the hyperpermeability in cultured HMVECs subjected to DDAVP and MRSA.

To further understand the downstream mechanisms of how V_2R activation causes the release of angiopoietin-2, we executed a multi-gene array profiling to determine the expression of the key G-protein coupled receptors (GPCRs). Surprisingly, none of the measured genes involved in the MAPK pathway was upregulated by DDAVP or MRSA in cultured HMVECs, suggesting that V_2R activation-induced angiopoietin-2 release is not mediated by the MAPK pathway. However, we found that the phospholipase C beta-4 (PLCβ4) gene was upregulated in these cells after DDAVP or MRSA treatment. PLCβ enzyme is a target molecule of the Gq subunits. Its activation catalyzes the formation of diacylglycerol (DAG) and inositol 1,4,5-trisphosphate (IP3) from the cleavage of phosphatidylinositol 4,5-bisphosphate (PIP_2). IP3 is directly involved in the release of intracellular calcium (47). Even though V_2R activation is coupled to Gs but not Gq subunits (48), it has been shown that V_2R has a particular ability to activate PLC in a Gq independent manner (49). Therefore, we speculate that in endothelial cells, V_2R may use cAMP as a secondary messenger along with IP3 and calcium. Additionally, it is well known that both tissue plasminogen activator (TPA) and angiopoietin-2 are common residents of the WPBs (50), and Muldowney *et al.* demonstrated that the release of TPA in endothelial cells is mediated by PLCβ (51). Therefore, the release of angiopoietin-2 may occur in a PLCβ-dependent manner.

Other important intermediates such as p38MAPK, AP-1, JNK, and ERK1 also have a role in the regulation of endothelial function (52, 53), and we first speculated that those intermediates might participate in the V_2R activation-induced angiopoietin-2 release. However, the multi-gene expression analysis showed no upregulation of *p38MAPK, AP-1, JNK or ERK1* at either 30 minutes, 1 hour, 3 hours or 6 hours of DDAVP or MRSA treatment.

The most updated sepsis guidelines underline, as an essential component in the criteria, the requirement of vasopressors to maintain a MAP >65mmhg despite adequate fluid resuscitation (54). As shown here, our model exhibits sepsis in just 6 hours postinjury and refractory hypotension progresses in the following time points. Although the fact that we did not employed a vasopressor may limit our results, previously we challenged our model with the vasopressor norepinephrine and we validated the development of organ failure and septic shock with a modified SOFA score showing significant worsening of both while on vasopressors (21).

It is imperative to mention that our study was not designed to evaluate this drug's efficacy to treat septic shock; nonetheless, the impressive outcome allows us to speculate that TLVP possesses an overall therapeutic benefit for this condition. Specifically, TLVP could limit the extravasation of fluids on an early stage and/or help eliminating excessed fluids posterior to aggressive fluid resuscitation. Either of these effects would impact reducing tissue edema, tissue hypoxia, multiorgan failure and mortality. In this regard, the ultimate translational goal will be utilizing these findings to design and conduct a small prospective clinical trial to evaluate this concept.

Taken together, our results indicate that V_2R activation during sepsis causes microvascular hyperpermeability and such effect is likely mediated through the V_2R/PLCβ4/angiopoietin-2 axis. In this regard, V_2R activation dynamics may directly impact the outcome of septic patients, particularly in those with severe fluid retention and tissue edema.

Supplementary Material

Refer to Web version on PubMed Central for supplementary material.

Acknowledgments

Funding Sources: National Institute of Health (grant no. RO1GM097480, PI: Enkhbaatar, P)

List of abbreviations:

ANGPT2	angiopoietin-2 gene
AVP	arginine vasopressin
CFU/mL	colony forming units per mL
COHb	carboxyhemoglobin
C_T	threshold cycle
CVP	central venous pressure
DDAVP	desmopressin
DMSO	dimethyl sulfoxide
HMVECs	microvascular endothelial cells
HR	heart rate
IP3	inositol 1,4,5-trisphosphate
LAP	left atrium pressure
LDH	lactate dehydrogenase
LR	lactated Ringer's
MAP	mean arterial pressure

MOI	multiplicity of infection
MRSA	Methicillin-resistant Staphylococcus Aureus
NS	normal saline
OD	optical density
OI	oxygenation index
PAP	pulmonary artery pressure
P_{aw}	airway pressure
PcP	pulmonary microvascular capillary pressure
PLCβ4	phospholipase C beta-4 gene
RT-qPCR	real-time polymerase chain reaction
SI	smoke inhalation
TLVP	tolvaptan
TPA	tissue plasminogen activator
vWF	von Willebrand factor
WBC	white blood cells
W/D	wet-to-dry ratio
WPBs	Weibel Palade bodies

REFERENCES

1. Adhikari NK, Fowler RA, Bhagwanjee S, Rubenfeld GD. Critical care and the global burden of critical illness in adults. Lancet. 2010;376(9749):1339–1346. [PubMed: 20934212]
2. Lagu T, Rothberg MB, Shieh MS, Pekow PS, Steingrub JS, Lindenauer PK. Hospitalizations, costs, and outcomes of severe sepsis in the United States 2003 to 2007. Crit Care Med. 2012;40(3):754–761. [PubMed: 21963582]
3. Angus D, Linde-Zwirble W, Lidicker J, Clermont G, Carcillo J, Pinsky M. Epidemiology of severe sepsis in the United States: analysis of incidence, outcome, and associated costs of care. Critical care medicine. 2001;29(7):1303–1310. [PubMed: 11445675]
4. Esteban A, Frutos-Vivar F, Ferguson ND, Penuelas O, Lorente JA, Gordo F, Honrubia T, Algora A, Bustos A, Garcia G, Diaz-Reganon IR, de Luna RR. Sepsis incidence and outcome: contrasting the intensive care unit with the hospital ward. Crit Care Med. 2007;35(5):1284–1289. [PubMed: 17414725]
5. Alberti C, Brun-Buisson C, Burchardi H, Martin C, Goodman S, Artigas A, Sicignano A, Palazzo M, Moreno R, Boulme R, Lepage E, Le Gall JR. Epidemiology of sepsis and infection in ICU patients from an international multicentre cohort study. Intensive care medicine. 2002;28(2):108–121. [PubMed: 11907653]
6. Martin GS. Sepsis, severe sepsis and septic shock: changes in incidence, pathogens and outcomes. Expert review of anti-infective therapy. 2012;10(6):701–706. [PubMed: 22734959]
7. Opal SM, van der Poll T. Endothelial barrier dysfunction in septic shock. J Intern Med. 2015;277(3):277–293. [PubMed: 25418337]

8. Russell J, Walley K, Singer J, Gordon A, Hébert P, Cooper D, Holmes C, Mehta S, Granton J, Storms M, Cook D, Presneill J, Ayers D, Investigators V. Vasopressin versus norepinephrine infusion in patients with septic shock. The New England journal of medicine. 2008;358(9):877–887. [PubMed: 18305265]
9. Vincent JL. Emerging therapies for the treatment of sepsis. Current opinion in anaesthesiology. 2015;28(4):411–416. [PubMed: 26087275]
10. Maybauer MO, Maybauer DM, Enkhbaatar P, Laporte R, Wisniewska H, Traber LD, Lin CD, Fan JJ, Hawkins HK, Cox RA, Wisniewski K, Schteingart CD, Landry DW, Riviere PJM, Traber DL. The Selective Vasopressin Type 1a Receptor Agonist Selepressin (FE 202158) Blocks Vascular Leak in Ovine Severe Sepsis. Critical Care Medicine. 2014;42(7):E525–E533. [PubMed: 24674922]
11. van der Heijden M, Pickkers P, van Nieuw Amerongen GP, van Hinsbergh VW, Bouw MP, van der Hoeven JG, Groeneveld AB. Circulating angiopoietin-2 levels in the course of septic shock: relation with fluid balance, pulmonary dysfunction and mortality. Intensive care medicine. 2009;35(9):1567–1574. [PubMed: 19551369]
12. Fisher J, Douglas JJ, Linder A, Boyd JH, Walley KR, Russell JA. Elevated Plasma Angiopoietin-2 Levels Are Associated With Fluid Overload, Organ Dysfunction, and Mortality in Human Septic Shock. Crit Care Med. 2016;44(11):2018–2027. [PubMed: 27441903]
13. Rondaij MG, Bierings R, Kragt A, van Mourik JA, Voorberg J. Dynamics and plasticity of Weibel-Palade bodies in endothelial cells. Arteriosclerosis, thrombosis, and vascular biology. 2006;26(5):1002–1007.
14. Kaufmann J, Oksche A, Wollheim C, Günther G, Rosenthal W, Vischer U. Vasopressin-induced von Willebrand factor secretion from endothelial cells involves V2 receptors and cAMP. The Journal of clinical investigation. 2000;106(1):107–116. [PubMed: 10880054]
15. Reif GA, Yamaguchi T, Nivens E, Fujiki H, Pinto CS, Wallace DP. Tolvaptan inhibits ERK-dependent cell proliferation, Cl(−) secretion, and in vitro cyst growth of human ADPKD cells stimulated by vasopressin. Am J Physiol Renal Physiol. 2011;301(5):F1005–1013. [PubMed: 21816754]
16. Ripoll GV, Garona J, Pifano M, Farina HG, Gomez DE, Alonso DF. Reduction of tumor angiogenesis induced by desmopressin in a breast cancer model. Breast cancer research and treatment. 2013;142(1):9–18. [PubMed: 24122393]
17. Fujiwara O, Fukuda S, Lopez E, Zeng Y, Niimi Y, DeWitt DS, Herndon DN, Prough DS, Enkhbaatar P. Peroxynitrite decomposition catalyst reduces vasopressin requirement in ovine MRSA sepsis. Intensive Care Med Exp. 2019;7(1):12. [PubMed: 31512009]
18. Enkhbaatar P, Joncam C, Traber L, Nakano Y, Wang J, Lange M, Connelly R, Kulp G, Saunders F, Huda R, Cox R, Schmalstieg F, Herndon D, Traber D. Novel ovine model of methicillin-resistant Staphylococcus aureus-induced pneumonia and sepsis. Shock (Augusta, Ga). 2008;29(5):642–649.
19. Enkhbaatar P, Zhu Y, Traber L, Traber D. Interplay between angiopoietin-2, vascular endothelial growth factor and peroxynitrite is an important determinant of vascular hyperpermeability during methicillin-resistant Staphylococcus aureus sepsis. Critical Care. 2011;15(S3).
20. Maybauer DM, Maybauer MO, Szabo C, Westphal M, Traber LD, Enkhbaatar P, Murthy KG, Nakano Y, Salzman AL, Herndon DN, Traber DL. Lung-protective effects of the metalloporphyrinic peroxynitrite decomposition catalyst WW-85 in interleukin-2 induced toxicity. Biochem Biophys Res Commun. 2008;377(3):786–791. [PubMed: 18951875]
21. Fukuda S, Ihara K, Andersen CR, Randolph AC, Nelson CL, Zeng Y, Kim J, DeWitt DS, Rojas JD, Koutrouvelis A, Herndon DN, Prough DS, Enkhbaatar P. Modulation of Peroxynitrite Reduces Norepinephrine Requirements in Ovine MRSA Septic Shock. Shock. 2019;52(5):e92–e99. [PubMed: 30499879]
22. Asmussen S, Ito H, Traber DL, Lee JW, Cox RA, Hawkins HK, McAuley DF, McKenna DH, Traber LD, Zhuo H, Wilson J, Herndon DN, Prough DS, Liu KD, Matthay MA, Enkhbaatar P. Human mesenchymal stem cells reduce the severity of acute lung injury in a sheep model of bacterial pneumonia. Thorax. 2014;69(9):819–825. [PubMed: 24891325]
23. Jonkam C, Zhu Y, Jacob S, Rehberg S, Kraft E, Hamahata A, Nakano Y, Traber LD, Herndon DN, Traber DL, Hawkins HK, Enkhbaatar P, Cox RA. Muscarinic receptor antagonist therapy improves

acute pulmonary dysfunction after smoke inhalation injury in sheep. Crit Care Med. 2010;38(12):2339–2344. [PubMed: 20838334]

24. Jean SS, Chang YC, Lin WC, Lee WS, Hsueh PR, Hsu CW. Epidemiology, Treatment, and Prevention of Nosocomial Bacterial Pneumonia. J Clin Med. 2020;9(1).
25. Rehberg S, Enkhbaatar P, Rehberg J, La E, Ferdyan N, Qi S, Wisniewski K, Traber L, Schteingart C, Rivière P, Laporte R, Traber D. Unlike arginine vasopressin, the selective V1a receptor agonist FE 202158 does not cause procoagulant effects by releasing von Willebrand factor. Critical care medicine. 2012;40(6):1957–1960. [PubMed: 22488005]
26. Miyazaki T, Sakamoto Y, Yamashita T, Ohmoto K, Fujiki H. Anti-edematous effects of tolvaptan in experimental rodent models. Cardiovascular drugs and therapy / sponsored by the International Society of Cardiovascular Pharmacotherapy. 2011;25 Suppl 1:S77–82.
27. Onogawa T, Sakamoto Y, Nakamura S, Nakayama S, Fujiki H, Yamamura Y. Effects of tolvaptan on systemic and renal hemodynamic function in dogs with congestive heart failure. Cardiovascular drugs and therapy / sponsored by the International Society of Cardiovascular Pharmacotherapy. 2011;25 Suppl 1:S67–76.
28. Lange M, Hamahata A, Traber DL, Cox RA, Kulp GA, Nakano Y, Traber LD, Herndon DN, Enkhbaatar P. Preclinical evaluation of epinephrine nebulization to reduce airway hyperemia and improve oxygenation after smoke inhalation injury. Crit Care Med. 2011;39(4):718–724. [PubMed: 21263320]
29. Lopez E, Fujiwara O, Lima-Lopez F, Suman OE, Mlcak RP, Hawkins HK, Cox RA, Herndon DN, Prough DS, Enkhbaatar P. Nebulized Epinephrine Limits Pulmonary Vascular Hyperpermeability to Water and Protein in Ovine With Burn and Smoke Inhalation Injury. Crit Care Med. 2016;44(2):e89–96. [PubMed: 26465218]
30. Nguyen U, Squaglia N, Boge A, Fung PA. The Simple Western™: a gel-free, blot-free, hands-free Western blotting reinvention. Nature Methods. 2011;8. [PubMed: 22205510]
31. Martins-Green M, Petreaca M, Yao M. An Assay System for In Vitro Detection of Permeability in Human “Endothelium”. 2008;443:137–153.
32. Lopez E, Peng Z, Kozar RA, Cao Y, Ko TC, Wade CE, Cardenas JC. Antithrombin III Contributes to the Protective Effects of Fresh Frozen Plasma Following Hemorrhagic Shock by Preventing Syndecan-1 Shedding and Endothelial Barrier Disruption. Shock. 2020;53(2):156–163. [PubMed: 31389906]
33. Gero D, Modis K, Nagy N, Szoleczky P, Toth ZD, Dorman G, Szabo C. Oxidant-induced cardiomyocyte injury: identification of the cytoprotective effect of a dopamine 1 receptor agonist using a cell-based high-throughput assay. International journal of molecular medicine. 2007;20(5):749–761. [PubMed: 17912470]
34. Van Deun J, Mestdagh P, Sormunen R, Cocquyt V, Vermaelen K, Vandesompele J, Bracke M, De Wever O, Hendrix A. The impact of disparate isolation methods for extracellular vesicles on downstream RNA profiling. Journal of extracellular vesicles. 2014;3.
35. Lopez E, Fujiwara O, Lima-Lopez F, Suman OE, Mlcak RP, Hawkins HK, Cox RA, Herndon DN, Prough DS, Enkhbaatar P. Nebulized Epinephrine Limits Pulmonary Vascular Hyperpermeability to Water and Protein in Ovine With Burn and Smoke Inhalation Injury. Critical Care Medicine. 2015:1.
36. Vincent JL, Sakr Y, Sprung CL, Ranieri VM, Reinhart K, Gerlach H, Moreno R, Carlet J, Le Gall JR, Payen D, Sepsis Occurrence in Acutely Ill Patients I. Sepsis in European intensive care units: results of the SOAP study. Crit Care Med. 2006;34(2):344–353. [PubMed: 16424713]
37. Rehberg S, Yamamoto Y, Sousse L, Bartha E, Jonkam C, Hasselbach A, Traber L, Cox R, Westphal M, Enkhbaatar P, Traber D. Selective V(1a) agonism attenuates vascular dysfunction and fluid accumulation in ovine severe sepsis. American journal of physiology Heart and circulatory physiology. 2012;303(10):54.
38. He X, Su F, Taccone FS, Laporte R, Kjolbye AL, Zhang J, Xie K, Moussa MD, Reinheimer TM, Vincent JL. A Selective V1A Receptor Agonist, Selepressin, Is Superior to Arginine Vasopressin and to Norepinephrine in Ovine Septic Shock. Crit Care Med. 2015.

39. Costello-Boerrigter LC, Boerrigter G, Cataliotti A, Harty GJ, Burnett JC Jr. Renal and anti-aldosterone actions of vasopressin-2 receptor antagonism and B-type natriuretic peptide in experimental heart failure. Circulation Heart failure. 2010;3(3):412–419. [PubMed: 20176717]
40. Watanabe K, Dohi K, Sugimoto T, Yamada T, Sato Y, Ichikawa K, Sugiura E, Kumagai N, Nakamori S, Nakajima H, Hoshino K, Machida H, Okamoto S, Onishi K, Nakamura M, Nobori T, Ito M. Short-term effects of low-dose tolvaptan on hemodynamic parameters in patients with chronic heart failure. Journal of cardiology. 2012;60(6):462–469. [PubMed: 23068288]
41. David S, Mukherjee A, Ghosh C, Yano M, Khankin E, Wenger J, Karumanchi S, Shapiro N, Parikh S. Angiopoietin-2 may contribute to multiple organ dysfunction and death in sepsis*. Critical care medicine. 2012;40(11):3034–3041. [PubMed: 22890252]
42. van Meurs M, Kumpers P, Ligtenberg JJ, Meertens JH, Molema G, Zijlstra JG. Bench-to-bedside review: Angiopoietin signalling in critical illness - a future target? Crit Care. 2009;13(2):207. [PubMed: 19435476]
43. Palud A, Parmentier-Decrucq E, Pastre J, De Freitas Caires N, Lassalle P, Mathieu D. Evaluation of endothelial biomarkers as predictors of organ failures in septic shock patients. Cytokine. 2015;73(2):213–218. [PubMed: 25794660]
44. Ong SP, Ng ML, Chu JJ. Differential regulation of angiopoietin 1 and angiopoietin 2 during dengue virus infection of human umbilical vein endothelial cells: implications for endothelial hyperpermeability. Medical microbiology and immunology. 2013;202(6):437–452. [PubMed: 23989887]
45. Gutbier B, Neuhauss AK, Reppe K, Ehrler C, Santel A, Kaufmann J, Scholz M, Weissmann N, Morawietz L, Mitchell TJ, Aliberti S, Hippenstiel S, Suttorp N, Witzenrath M, Capnetz, dagger PSGd. Prognostic and Pathogenic Role of Angiopoietin-1 and −2 in Pneumonia. Am J Respir Crit Care Med. 2018;198(2):220–231. [PubMed: 29447449]
46. Ghosh CC, Thamm K, Berghelli AV, Schrimpf C, Maski MR, Abid T, Milam KE, Rajakumar A, Santel A, Kielstein JT, Ahmed A, Thickett D, Wang K, Chase M, Donnino MW, Aird WC, Haller H, David S, Parikh SM. Drug Repurposing Screen Identifies Foxo1-Dependent Angiopoietin-2 Regulation in Sepsis. Crit Care Med. 2015;43(7):e230–240. [PubMed: 25855898]
47. Sandal M, Paltrinieri D, Carloni P, Musiani F, Giorgetti A. Structure/Function Relationships of Phospholipases C Beta. Current protein & peptide science. 2013;14(8):650–657. [PubMed: 24384033]
48. Wu S, Birnbaumer M, Guan ZQ. Phosphorylation analysis of G protein-coupled receptor by mass spectrometry: Identification of a phosphorylation site in V2 vasopressin receptor. Analytical Chemistry. 2008;80(15):6034–6037. [PubMed: 18578504]
49. Zhu X, Birnbaumer L. G protein subunits and the stimulation of phospholipase C by Gs-and Gi-coupled receptors: Lack of receptor selectivity of Galpha(16) and evidence for a synergic interaction between Gbeta gamma and the alpha subunit of a receptor activated G protein. Proc Natl Acad Sci U S A. 1996;93(7):2827–2831. [PubMed: 8610126]
50. Kaufmann JE, Vischer UM. Cellular mechanisms of the hemostatic effects of desmopressin (DDAVP). Journal of Thrombosis and Haemostasis. 2003;1(4):682–689. [PubMed: 12871401]
51. Muldowney JAS, Painter CA, Sanders-Bush E, Brown NJ, Vaughan DE. Acute tissue-type plasminogen activator release in human microvascular endothelial cells: The roles of Gαq, PLC-β, IP3 and 5,6-epoxyeicosatrienoic acid. Thrombosis and Haemostasis. 2007.
52. Kaur J, Woodman RC, Kubes P. P38 MAPK: critical molecule in thrombin-induced NF-kappa B-dependent leukocyte recruitment. American journal of physiology Heart and circulatory physiology. 2003;284(4):H1095–1103. [PubMed: 12505871]
53. Ye F-C, Blackbourn D, Mengel M, Xie J-P, Qian L-W, Greene W, Yeh IT, Graham D, Gao S-J. Kaposi's sarcoma-associated herpesvirus promotes angiogenesis by inducing angiopoietin-2 expression via AP-1 and Ets1. Journal of virology. 2007;81(8):3980–3991. [PubMed: 17287278]
54. Singer M, Deutschman CS, Seymour CW, Shankar-Hari M, Annane D, Bauer M, Bellomo R, Bernard GR, Chiche JD, Coopersmith CM, Hotchkiss RS, Levy MM, Marshall JC, Martin GS, Opal SM, Rubenfeld GD, van der Poll T, Vincent JL, Angus DC. The Third International Consensus Definitions for Sepsis and Septic Shock (Sepsis-3). JAMA : the journal of the American Medical Association. 2016;315(8):801–810. [PubMed: 26903338]

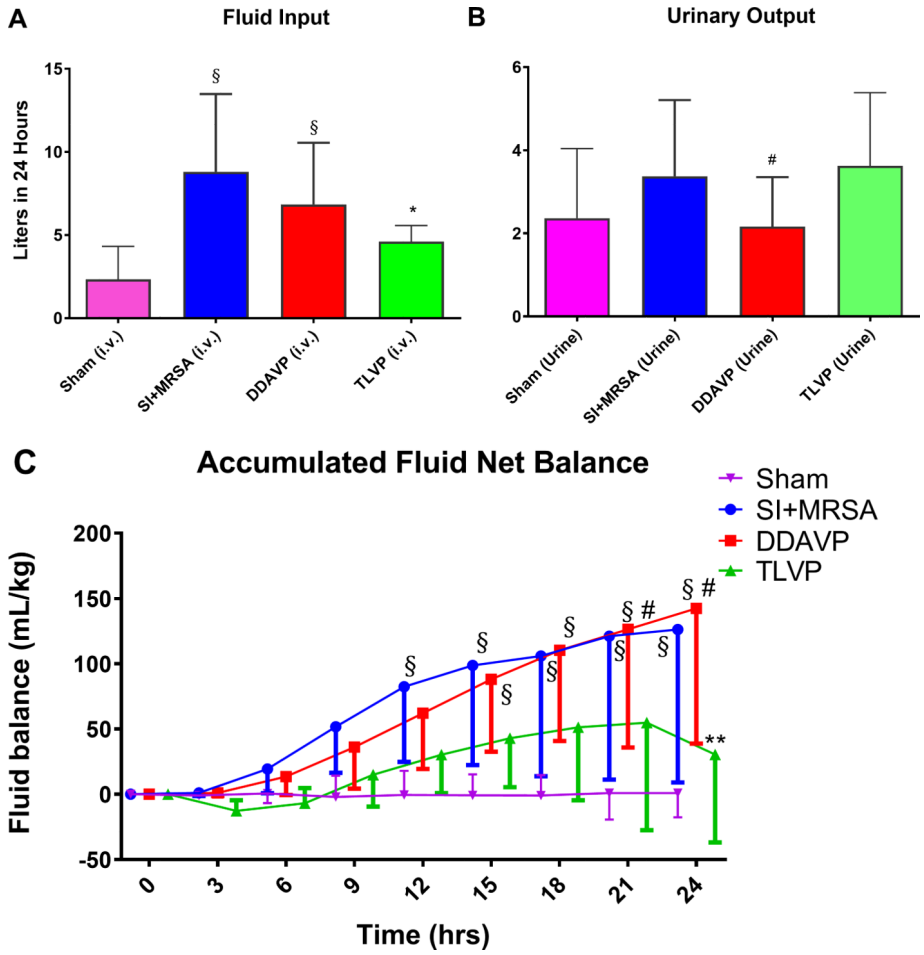

Figure 1: TLVP treatment prevents systemic fluid retention.

In vivo MRSA-induced sepsis model showing the different effects on fluid dynamics after treatment with tolvaptan (TLVP) or desmopressin (DDAVP) vs. no treatment (SI+MRSA) and no injured groups (Sham). (A) TLVP treatment significantly decreased the fluid requirement during sepsis (B) without having effects on urinary output. (C) As a result, SI +MRSA and DDAVP groups accumulated a large amount of fluids. TLVP treatment proved to be efficient in preventing this excessive amount of fluid retention during sepsis. The hematocrit was similar in all groups. Data are expressed as mean ± SD. *p <0.05 vs. SI +MRSA; #p <0.05 vs. TLVP; §p <0.05 vs. Sham.

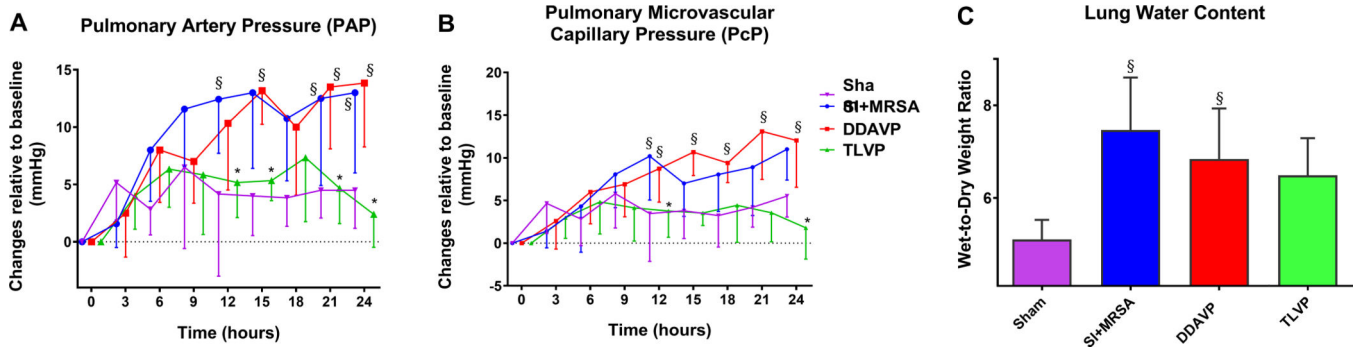

Figure 2: TLVP treatment attenuates pulmonary vascular damage and water retention.

In vivo pulmonary intravascular pressure assessment (by invasive monitoring) and water content estimation (by W/D ratio). Following septic insult, the pulmonary microvasculature was affected demonstrating by (A) elevated in pulmonary resistance and (B) pulmonary microvascular capillary pressure, and (C) water retention in the lung tissue. TLVP treatment ameliorated the three parameters. Data are expressed as mean ± SD. *p <0.05 vs. SI +MRSA; §p <0.05 vs. Sham.

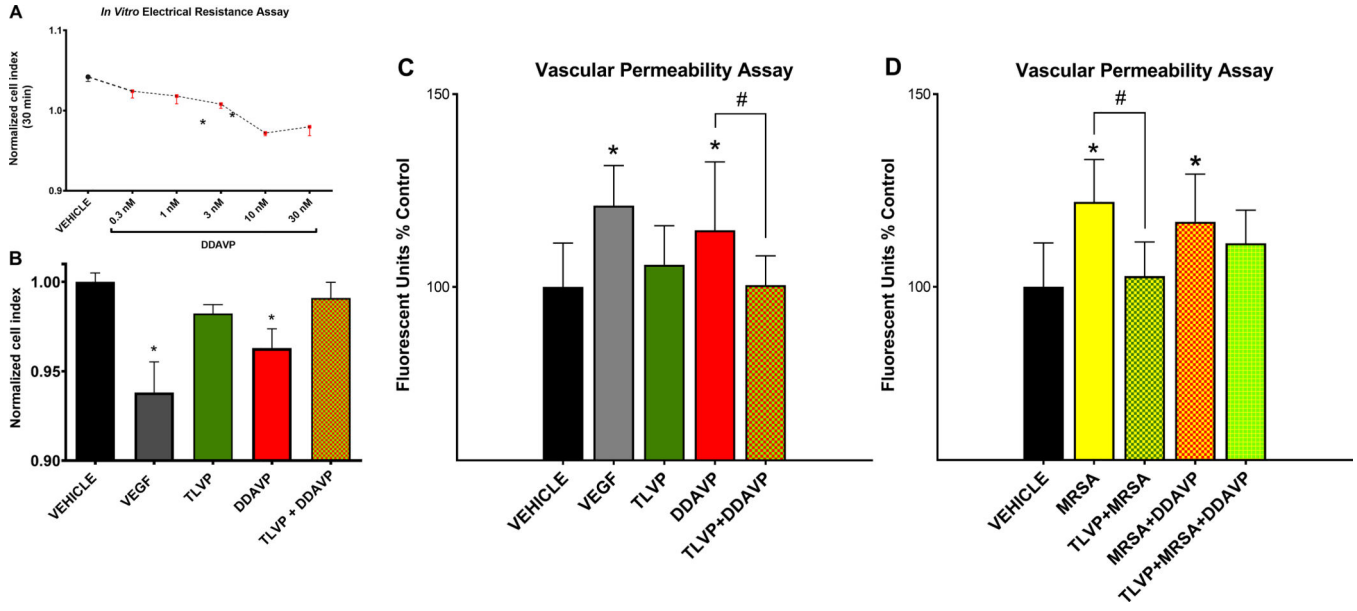

Figure 3: V_2R activation mediates the MRSA-induced endothelial hyperpermeability.

Changes in cell-cell dynamics and functional permeability in cultured HMVECs were assessed first by electrical resistance assay for time and dose evaluation. Next, the functional barrier was further evaluated using a vascular permeability assay. (A) DDAVP treatment decreased the electrical resistance in a dose-dependent fashion after a short, only 30-min-long, incubation period. (B) V_2R agonist, DDAVP, decreases the electrical impedance similar to the positive control VEGF. Pretreatment with TLVP prevents changes in electrical resistance. (C) V_2R agonist, DDAVP, increases the endothelial barrier permeability similar to the positive control VEGF. (D) MRSA also increases the endothelial barrier permeability. The V_2R antagonist, TLVP, attenuates the endothelial permeability induced by both insults (C and D). Data are expressed as mean ± SD. *p <0.05 vs. Vehicle; #p <0.05.

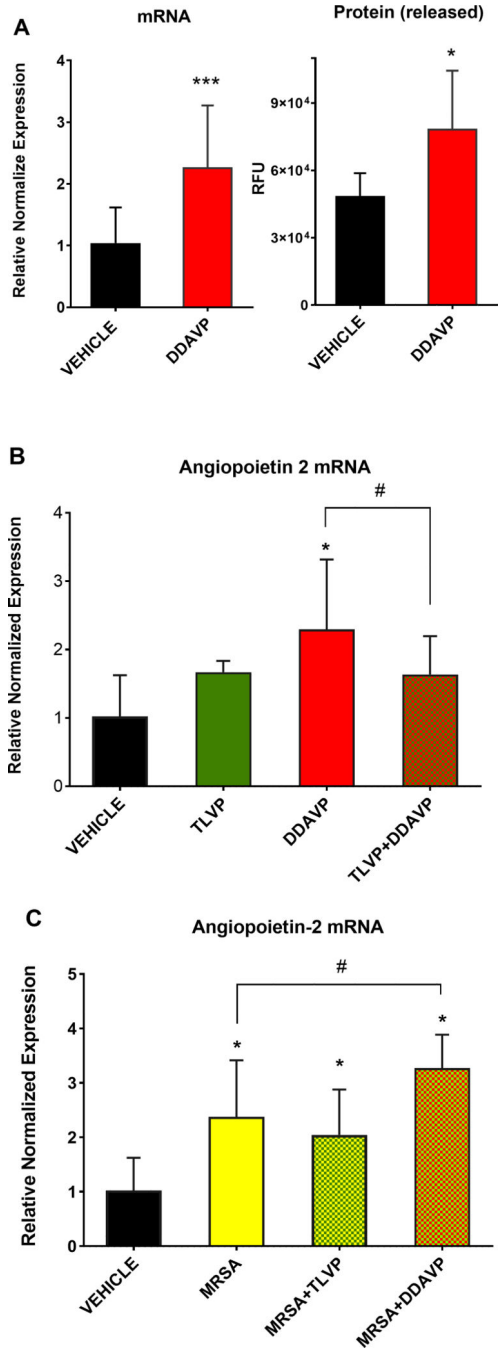

Figure 4: The expression of angiopoietin-2 increases after V_2R stimulation by V_2R agonism DDAVP and/or MRSA.

The expression of angiopoietin-2, a potent permeability factor, was measured in confluent HMVECs. First, (A) mRNA and protein were assessed after treatment with DDAVP to ensure that both mRNA and protein expression increase after V_2R stimulation. Subsequent experiments measuring angiopoietin-2 mRNA demonstrate that TLVP attenuates the angiopoietin-2 upregulation linked to V_2R agonism. (B) TLVP pretreatment attenuates the DDAVP-induced elevated mRNA expression of angiopoietin-2. (C) Likewise, MRSA-

induced increase in angiopoietin-2 is attenuated by TLVP and potentiated by DDAVP. Data are expressed as mean ± SD. *p <0.05 vs. Vehicle; #p <0.05.

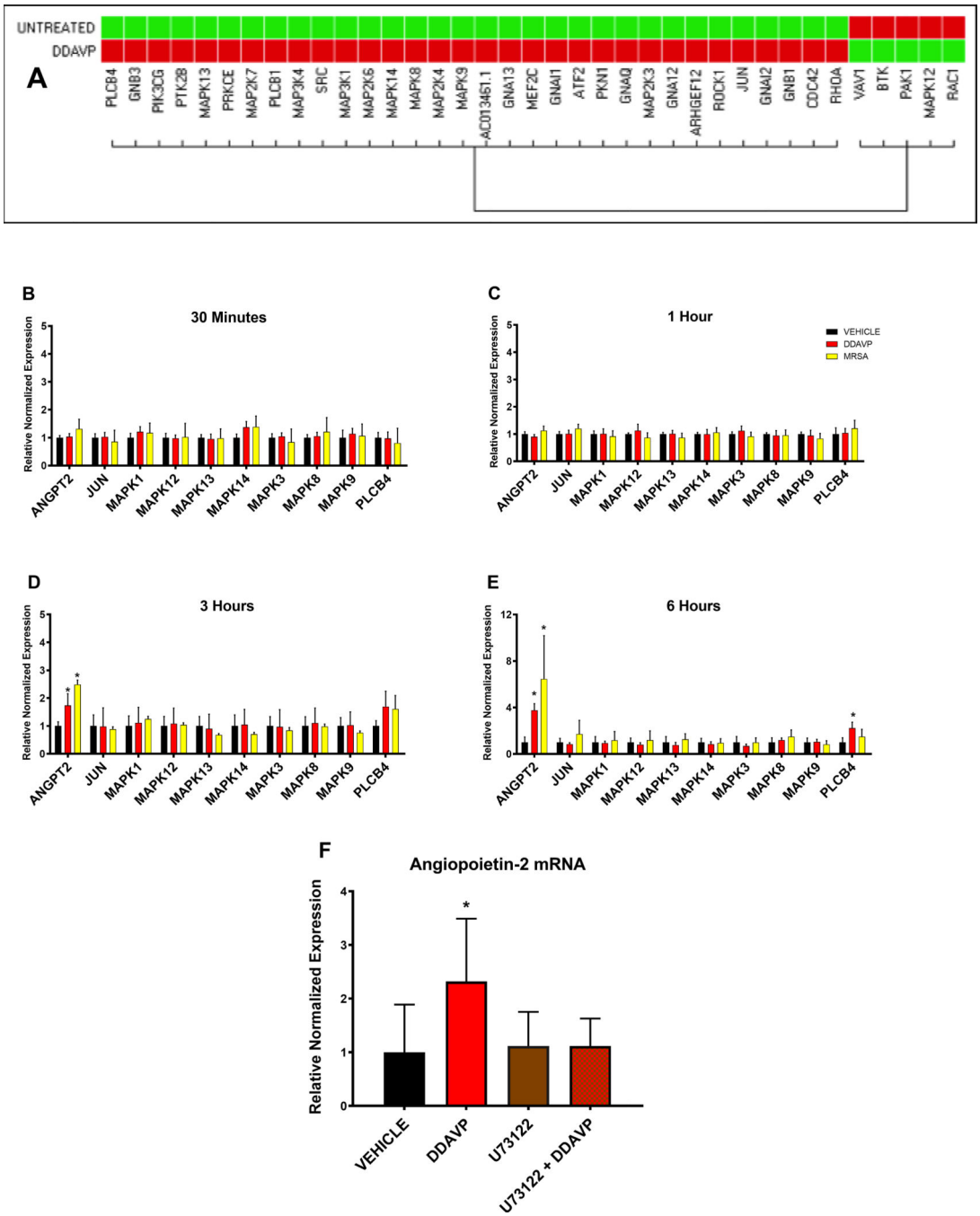

Figure 5: The rapid V_2R-induced angiopoietin-2 upregulation is mediated by PLCB and not by the activation of MAPK pathway.

(A) A screening G-protein-coupled multi-gene assay targeting 38 genes suggested that PLCB4 expression was significantly elevated by 2-hour-long V_2R stimulation. (B, C, D, and E) The lack of influence of the MAPK pathway and the PLCB4 upregulation was confirmed with DDAVP and MRSA treatment during 0.5, 1, 3, and 6 hours, n=3 for each group. (D) After 3 hours of treatment, we observed a slight increase in PLCB4 expression with both MRSA and DDAVP challenge and parallel to an increase in ANGPT2 (angiopoietin-2 gene) expression. (E) The PLCB4 upregulation was significant after 6 hours of DDAVP treatment.

In a subsequent experiment, cells were treated with U73122, a pharmacological inhibitor of PLCB, before the addition of DDAVP. As shown, (F) treatment with U73122 prevents the DDAVP-induced upregulation of ANGPT2. Data are expressed as mean ± SD. *p <0.05 vs. Vehicle.